Correction of Proton Resonance Frequency Shift Temperature Maps for Magnetic Field Disturbances Using Fat Signal

A. V. Shmatukha[1], P. R. Harvey[2], C. J. Bakker[3]

[1]Image Sciences Institute, University Medical Center Utrecht, Utrecht, Netherlands, [2]MR CTO Office, Business Unit MR, Philips Medical Systems, Best, Netherlands, [3]Radiology Department, University Medical Center Utrecht, Utrecht, Netherlands

INTRODUCTION: The ability to measure small temperature changes with high accuracy using MRI has many potential clinical applications – for instance, specific absorption rate management or thermal ablation guidance. The accuracy of the Proton Resonance Frequency Shift (PRFS) method of MRI temperature mapping is handicapped by the method's sensitivity to magnetic field disturbance that are misinterpreted as artifact temperature changes. The disturbances can arise, for instance, from hardware drifts, subject motion or tissue perfusion and susceptibility changes with temperature. If not compensated, the resulting temperature artifacts can completely obscure the true temperature estimation, especially if temperature elevations are small. As the fat protons experience the same magnetic field disturbances as the water protons but no temperature-related frequency shift, the fat signal can be used for correcting PRFS temperature maps for the disturbances (1, 2). We propose a simpler correction method that has better compensation capability as well as higher spatial and temporal resolution than the previously reported ones (1, 2).

THEORY: The proposed Triple Spin-Gradient Echo (TSGE) pulse sequence acquires two GRE read-outs within one SE TR before and after the RF echo (Fig. 1). This enables obtaining three temperature estimations (instead of one in the traditional approach – 3, 4). TSGE is run using interleaved water- and fat-selective scans. Suppose, $\mathbf{S}_w^1$, $\mathbf{S}_w^2$, $\mathbf{S}_f^1$, $\mathbf{S}_f^2$ are complex reconstructed pixel signals acquired during water- and fat- selective scans at the first and second read-outs. The phase difference maps $\mathbf{P}_1 = \tilde{\mathbf{S}}_w^1 \times \left(\tilde{\mathbf{S}}_f^1\right)^* \times \left(\mathbf{S}_w^1 \times \left(\mathbf{S}_f^1\right)^*\right)^*$ [1], $\mathbf{P}_2 = \tilde{\mathbf{S}}_w^2 \times \left(\tilde{\mathbf{S}}_f^2\right)^* \times \left(\mathbf{S}_w^2 \times \left(\mathbf{S}_f^2\right)^*\right)^*$ [2] and $\mathbf{P}_3 = \tilde{\mathbf{S}}_w^2 \times \left(\tilde{\mathbf{S}}_f^2\right)^* \times \left(\tilde{\mathbf{S}}_w^1 \times \left(\tilde{\mathbf{S}}_f^1\right)^*\right)^* \times \left(\mathbf{S}_w^2 \times \left(\mathbf{S}_f^2\right)^* \times \left(\mathbf{S}_w^1 \times \left(\mathbf{S}_f^1\right)^*\right)^*\right)^*$ [3] are re-calculated into degrees Celsius and averaged to obtain the resulting temperature map (the wave sign above denotes the identical signal acquired after temperature changes). Alternatively, the linear regression could be performed on them (5).

METHODS: MRI was performed on 1.5T Intera-NT (Philips MS) using birdcage and surface coils on a 0.5-kg box of a bread spread containing 35% of fat (Bewust Light, Albert Hein, The Netherlands). The TSGE pulse sequence was simulated by SE EPI. Nine EPI read-outs were acquired around an RF echo and reconstructed separately. The first and last ones were used in post-processing. During a field disturbance experiment, a hollow cylinder made from a non-ferromagnetic alloy was moved inside the scanner bore in-between image acquisitions to create the disturbances. Two 7mm- thick slices were acquired in 42.0 sec. with in-plane spatial resolution of 1.07x1.07 mm using TR /TE1 /TE2 /RFTE /NSA = 150 ms /11.19 ms /23.31 ms /18.0 ms /6. During a motion experiment, the box was moved 152.4 mm away from its initial position and back in both sides in steps of 76.2 mm. During a motion with field disturbances experiment, the box was imaged twice in each position and a water-filled bottle was placed into the scanner bore before the second image acquisition to create the disturbances. Two 7mm- thick slices were acquired in 33.9 sec. with in-plane spatial resolution of 1.09x1.07 mm using TR /TE1 /TE2 /RFTE /NSA = 150 ms /12.15 ms /22.52 ms /18.0 ms /6. During the laser hearing experiment, the spread was first frozen to ~0°C and then heated up using a diode array laser (Diomed Ltd., Cambridge, UK). Its temperature was measured with a fluoroptic thermometer (Luxtron Corp., Santa Clara, CA, USA). Two 6mm- thick slices were acquired in 18.3 sec. with in-plane spatial resolution of 1.25x1.25 mm using TR /TE1 /TE2 /RFTE /NSA = 155 ms /12.16 ms /22.54 ms /18.0 ms /4. Image processing was performed using IDL V.6.1. For the purpose of comparison, the Chemical Shift Selective Phase Mapping temperature estimation (CSSPM, 1) was simulated via $\tilde{\mathbf{S}}_w^2 \times \left(\tilde{\mathbf{S}}_f^2\right)^*$ as well as The Spin Echo – Gradient Echo temperature estimation (SEGE, 4) was simulated via $\tilde{\mathbf{S}}_w^2 \times \left(\tilde{\mathbf{S}}_w^0\right)^*$, where $\tilde{\mathbf{S}}_w^0$ is the closest to the RF echo read-out (shifted about RFTE by +0.625-0.677 msec).

RESULTS: Fig.2 depicts temperature artifacts due to the metal cylinder moving within the scanner bore toward the imaged phantom and away from it. Fig.3 depicts temperature artifacts due to inter-scan motion of the imaged phantom in the steps of 76.2 mm right and left from its initial position. Fig.4 depicts temperature artifacts due to imaged phantom motion combined with field disturbances created by positioning a water bottle nearby the phantom during the acquisition of the second image at each position. Our method has demonstrated much stronger immunity toward the magnetic field disturbances than other methods. Fig.5 depicts temperature measured during the laser heating with simultaneous field disturbances experiment. The temperatures estimated by PRFS and SEGE oscillate synchronously with water bottle repositioning because they are unable to compensate for the field disturbances. The temperature reported by our method is closer to those measured by the fluoroptic thermometer and deviates less during water bottle repositioning than the temperature reported by CSSPM.

CONCLUSIONS: As TSGE was simulated by another pulse sequence, the exact values of TE1 and TE2 were not known and estimated values were used in post-processing. We believe this was the reason why our method reported some small temperature artifacts. One must keep in mind, that the same estimated TE2 value was also used by the rest of the methods, so they performed in the equal conditions. Our method has been demonstrated to have superior immunity to magnetic field disturbances as compared to CSSPM and SEGE. Our method is simple to implement. Unlike the CSSPM method (1), it demands no special tuning operation to resolve the uncertainty error arising from the conversion from the phase difference to the chemical shift one. Unlike the spectroscopic method (2), it demands no sophisticated curve fitting. When TSGE is implemented as a separate pulse sequence, its SNR and temperature accuracy will be even higher. TSGE can be used for the guidance of thermal therapies involving tissues containing fat or surrounded by fat.

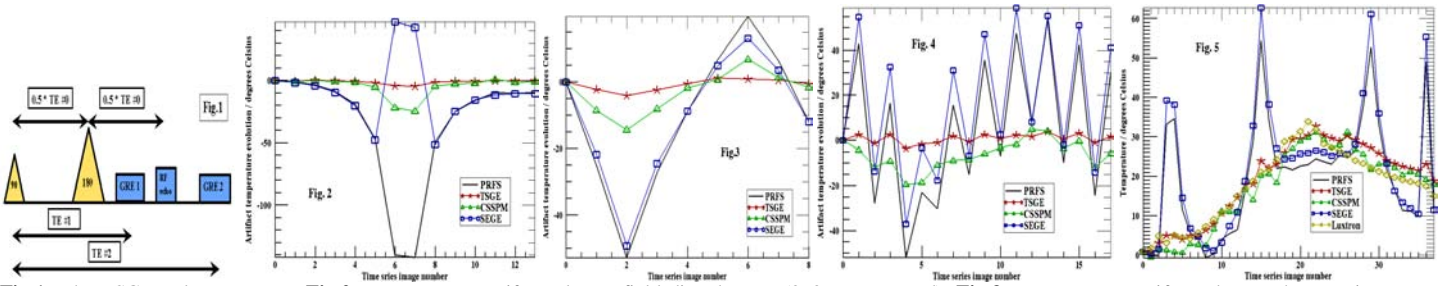

Fig.1: The TSGE pulse sequence. **Fig.2:** Temperature artifacts due to field disturbances (3x3 px averaged). **Fig.3:** Temperature artifacts due to phantom inter-scan motion (3x3 px averaged). **Fig.4:** Temperature artifacts due to combined motion and field disturbances (3x3 px averaged). **Fig.5:** Temperature evolution during laser heating (2x2 px averaged).

REFERENCES: **1.** K. Kuroda et al., MRM 38: 845-851 (1997). **2.** K. Kuroda et al., MRM 43: 220-225 (2000). **3.** Y. Ishihara et al., MRM 34: 814-823 (1995). **4.** T. Wu et al., Proc. Intl. Soc. Mag. Reson. Med. 10 (2002). **5.** R.V. Mulkern et al., JMRI 8: 493-502 (1998).